

ac and dc current-induced motion of a 360° domain wall

Mark D. Mascaro* and C. A. Ross†

Department of Materials Science and Engineering, Massachusetts Institute of Technology, Cambridge, Massachusetts 02139, USA

(Received 29 November 2010; published 10 December 2010)

The response of 360° domain walls in narrow magnetic stripes to applied dc and ac currents, investigated by micromagnetic simulation, differs qualitatively from the response of 180° domain walls. The 360° domain-wall velocity scales with a dc current but is independent of an applied magnetic field along the stripe. An annihilation process occurs at a critical dc current density that varies with the applied field. When a 360° wall is perturbed, it oscillates at a characteristic frequency in the gigahertz range which is tunable by the applied magnetic field, and an ac current applied at half the characteristic frequency excites a resonant response.

DOI: [10.1103/PhysRevB.82.214411](https://doi.org/10.1103/PhysRevB.82.214411)

PACS number(s): 75.60.Ch, 75.76.+j, 75.78.Fg, 75.78.Cd

Current-driven manipulation of transverse 180° domain walls (180DWs) in patterned in-plane magnetized thin-film stripes via the spin-torque effect is an essential component of domain-wall (DW) devices under development for memory¹ and logic^{2,3} applications. As a result, the response of 180DWs to an applied current has been investigated in detail.^{4–9} An applied field or current drives a 180DW along a magnetic stripe with a velocity that increases linearly with the field strength or current density until the wall reaches a velocity at which Walker breakdown occurs.^{7,10} Increasing the driving force beyond the breakdown limit sharply lowers the 180DW velocity, and a further increase recovers a linear driving force-velocity relationship, but with a smaller proportionality constant^{6,7,11} and with oscillations in the structure and velocity of the 180DW.^{12–16} There have also been studies of current-driven motion of arrays of 180DWs in a wire,^{1,17} in which the walls may move at different velocities and eventually impinge and annihilate.¹⁷

Despite the interest in 180DWs, there has been little exploration of the current-induced motion of 360° domain walls (360DWs), except in the ballistic case of ferromagnetic semiconductors.¹⁸ 360DWs are metastable structures which can be formed by the combination of two transverse 180DWs in which the magnetization directions at the centers of the 180DWs are oriented in opposite directions across the stripe.^{19–25} The response of 360DWs to applied fields has been well characterized. For example, a field applied along the stripe does not translate a 360DW, but instead compresses or expands it, ultimately collapsing or dissociating the wall, respectively.^{20,25,26} 360DWs are of considerable importance in thin-film devices, because of their effects on the subsequent magnetic reversal of the device, and the influence of their stray field on nearby magnetic structures or even other nearby DWs.^{23–25} Because coupling of 180DWs to form 360DWs is likely to occur in any DW device at sufficient DW density, understanding of the behavior of the 360DW is important for the development of DW devices. In this article we show that 360DWs exhibit qualitatively distinct current-driven behavior compared to that of 180DWs, including a strikingly different breakdown process that results in annihilation of the 360DW, and gigahertz (GHz)-range, field-tunable resonant behavior that can be excited by an applied ac current.

Current- and field-induced behavior of 360DWs was investigated using the dynamic NIST OOMMF 3D micromag-

netic solver.²⁷ The structure consisted of a 5048 nm × 100 nm × 5 nm NiFe (Permalloy) nanowire with 4 nm × 4 nm × 5 nm unit cells, in which the magnetization of a 48-nm-long region at each end of the stripe was fixed parallel to the stripe to provide boundary conditions. The exchange constant was $A=1.3 \times 10^{-6}$ erg/cm, the saturation magnetization was $M_s=860$ emu/cm³, the polarization factor was $P=0.4$, the anisotropy was zero, and the Gilbert damping parameter was $\alpha=0.01$. The nonadiabatic spin-torque term β (Refs. 11, 19, and 28) was varied between 0.02 and 0.05. An initial state was generated by relaxing a DW placed approximately 2 μ m from the left end of the stripe, by equilibrating the magnetization configuration such that no spin was rotating faster than 0.12°/ns. This DW location was chosen so that the influence of the stray field from the ends of the stripe was negligible. Initial 180DW and 360DW configurations are shown in Figs. 1(a) and 1(b). The locations of 360DWs as a function of time and the positions at which they annihilated were determined from the value of the transverse (y axis) component of the magnetization as a function of distance along the stripe.

The simulations show that 360DWs translate under an applied current, showing an approximately linear increase in velocity with current density. Figure 2(a) gives the velocity calculated at zero applied field as a function of spin current velocity u . The spin current velocity is proportional to the applied current density as $u=JPg\mu_B/(2eM_s)$, where J is the current density, and the $g\mu_B/(2eM_s)$ term in Permalloy is 7×10^{-11} m³/C.¹¹ At zero field the DW velocity for the 360DW is similar to that obtained for a 180DW for spin current velocities up to ~ 200 m/s. As this simulation is performed for nonzero β parameter and zero anisotropy in a geometrically perfect wire, there was no critical current density for DW motion.

Figure 2(b) shows the effect on DW velocity of a magnetic field applied along the stripe (x -axis field) for $u=80, 100, \text{ and } 120$ m/s for both a 180DW and a 360DW. The 180DW showed the expected Walker behavior in which the velocity increased with field then dropped abruptly at a field near 14 Oe. In contrast, the velocity of the 360DW had no detectable dependence on the field along the stripe in the range of -25 Oe to $+50$ Oe. Below -25 Oe, the 360DW dissociated to form a reverse domain, while at much higher positive fields (1438 Oe, not shown), the 360DW collapsed. The velocities of the 180DW and the 360DW were identical

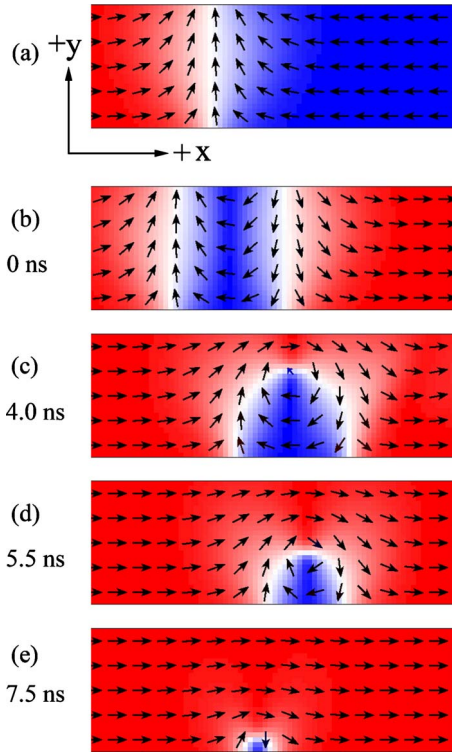


FIG. 1. (Color online) (a) Part of stripe showing the equilibrium transverse 180DW structure. Axes are indicated. (b) The equilibrium 360DW structure at zero field. (c) Part way through the annihilation process of a 360DW showing a reverse domain bounded by a U-shaped 180DW. [(d) and (e)] Successive snapshots of the 360DW annihilation process.

at zero applied field, consistent with Fig. 2(a), i.e., for moderate current densities (those below the current required to cause annihilation of the 360DW described below) a 360DW under any applied field propagated with the same velocity as a 180DW at zero field.

At a spin current density of $u=238$ m/s, the 360DW exhibited an annihilation process which is qualitatively different from the Walker breakdown exhibited by the 180DW at $u=400$ m/s at zero applied field. In agreement with prior work,¹²⁻¹⁴ Walker breakdown of the 180DW at high current or field occurred by the emission of an antivortex core from the stripe edge and an oscillation in the magnetic configuration and the velocity of the 180DW, but the 180DW was not destroyed. In contrast, the annihilation of the 360DW was an irreversible process which occurred by the creation of a vortex core at one edge of the stripe resulting in the formation of a single 180DW enclosing a U-shaped reverse domain on the other edge of the stripe, as shown in Fig. 1(c). At this point the velocity of the DW along the stripe fell to zero, and the U-shaped reverse domain contracted, Fig. 1(d). As the shrinking reverse domain approached the edge of the wire, it began to accelerate along $-x$, opposite to the initial propagation direction, Fig. 1(e). Eventually, the reverse domain vanished, releasing a burst of spin waves. The current-induced 360DW annihilation also differed from the annihilation process of a 360DW caused by a large field in the absence of a current, which occurs via the formation and movement of

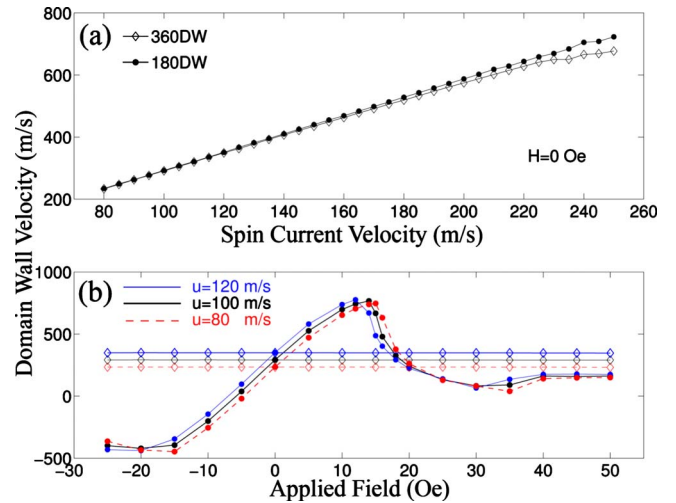


FIG. 2. (Color online) A comparison of domain-wall velocities for 360° and 180° domain walls (a) at zero applied field with varying spin current velocity and (b) at fixed-spin current velocity $u = 100$ m/s with varying applied field. The parameter $\beta=0.03$ in all cases. Positive field and velocity are directed to the right, along $+x$.

multiple vortex cores accompanied by the emission of spin waves.

Figure 3(a) summarizes the effects of spin current density and applied field on the 360DW for $\beta=0.03$. At low current densities, below $u=166$ m/s at zero applied field, the 360DW propagated at constant velocity until it reached the end of the stripe. When it collided with the fixed-spin region at the end of the stripe it showed damped oscillations but was not annihilated. At high current densities, above $u=237$ m/s at zero field, after propagating some distance along the stripe, the 360DW collapsed following the process described in Figs. 1(c)–1(e). At intermediate current densities the 360DW propagated until it reached the end of the stripe but collapsed once it reached the boundary. These three regimes are denoted stable propagation, perturbed annihilation, and spontaneous annihilation, respectively, in Fig. 3(a). Below -25 Oe, the 360DW dissociated but above -25 Oe increasing field compressed the 360DW and lowered the value of current density at which annihilation of the 360DW occurred, from $u=267$ m/s at -25 Oe to $u=201$ m/s at 50 Oe. An increasing applied field brought the component 180DWs closer together, facilitating the initial meeting of the 180DWs at the edge of the stripe which begins the annihilation process. It is expected that the critical current for breakdown would continue to decrease for increasing field, until the 360DW collapses spontaneously at 1438 Oe and zero current. Because the velocity of the 360DW is independent of field, the increase in critical current also increases the maximum propagation velocity. In contrast, a 180DW showed little effect of field on the propagation velocity at breakdown, although a *transverse* applied field has been shown to suppress breakdown and enable higher velocity.²⁹ These results illustrate qualitative differences between current-driven 180DW and 360DW behavior.

The nonadiabaticity parameter β had a significant influence on the critical current density for breakdown, as shown in Fig. 3(b). As β decreases, the critical current densities for

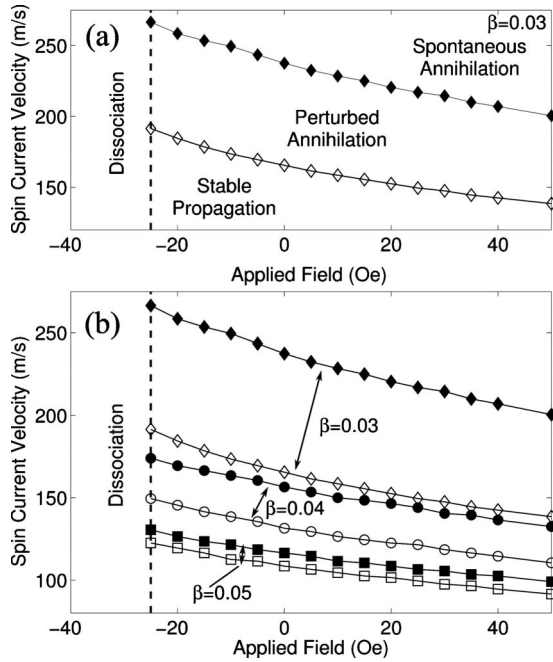


FIG. 3. (a) The behavior of a 360DW subjected to an applied field and dc current. Filled diamonds indicate the boundary between spontaneous and perturbed annihilation; open diamonds, between stable propagation and perturbed annihilation. (b) The behavior of a 360DW subjected to an applied field and dc current for varying values of β . Diamonds indicate $\beta=0.03$, circles indicate $\beta=0.04$, and squares indicate $\beta=0.05$. For each β value, filled symbols indicate the boundary between perturbed and spontaneous annihilation and open symbols the boundary between stable propagation and perturbed annihilation.

perturbed and spontaneous annihilation increase significantly, and the range of the perturbed annihilation regime increases. For $\beta=0.02$ no spontaneous annihilation was observed even at $u=350$ m/s, corresponding to a current density of 1.25×10^{13} A/m². This β dependence is in general agreement with previous work on 180DW motion, in which increasing β for $\beta > \alpha$ led to higher velocities at a given field, explained by the greater fieldlike torque provided by increasing β ,²⁸ as well as lower Walker breakdown velocities.¹¹

The foregoing results correspond to a Permalloy stripe with cross-sectional area 100×5 nm². Simulations of other geometries indicated that the results are quantitatively similar for stripes in which the 360DW equilibrium structure resembles that of Fig. 1(b), in which the cores of the two component 180DWs lie approximately antiparallel to each other. For example, changing the stripe width from 100 to 50 nm lowered the zero-field annihilation spin current density from $u=238$ m/s to $u=236$ m/s, and the DW velocity decreased from 435 to 429 m/s at $u=150$ m/s. However, for stripe widths above ~ 120 nm, the two component 180DWs developed mirror-image curvatures so that the equilibrated 360DW was narrower at one side of the stripe than the other, and the current required to annihilate the 360DW was lowered significantly.

We now describe the high-frequency behavior of the 360DW and show how its oscillation can be excited by an ac

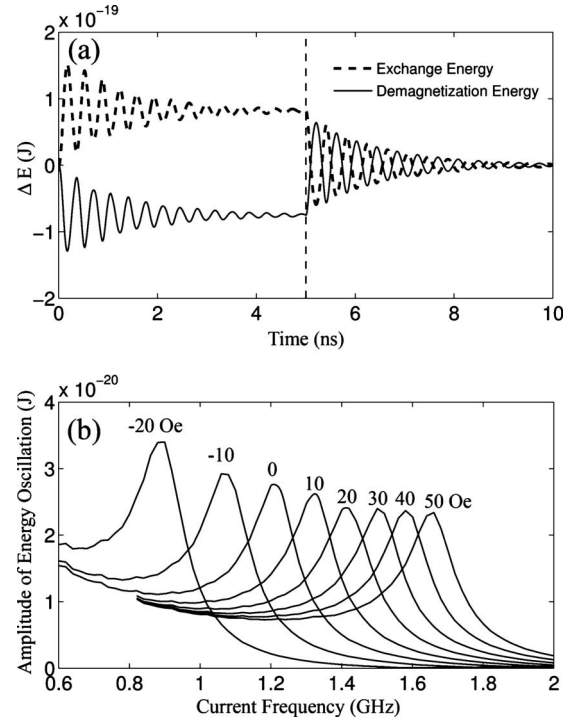


FIG. 4. (a) Oscillations in demagnetization (solid line) and exchange (dashed line) energies in a 360DW. A field of +20 Oe was applied at time=0 and removed at time=5 ns with no applied current. The vertical axis represents the difference in energy compared to its value at equilibrium in zero field. (b) Steady-state energy oscillation amplitude in a 360DW subjected to an applied field and current as a function of field strength and current frequency. The amplitude of the current was fixed at $u=240$ m/s or $J=8.57 \times 10^{12}$ A/m².

current. We note first that the 360DW displayed an excitation mode in which its length (i.e., the distance between the cores of the component 180DWs) oscillates but the position of its midpoint remains fixed; similar oscillatory behavior has been found for field-excited 360DWs in thin-film stripes³⁰ and thick films.³¹ We characterized this excitation by perturbing the 360DW with an applied field pulse and measuring the frequency of the resulting damped oscillations in the demagnetization and exchange energies, as shown in Fig. 4(a). This intrinsic resonance was observed in the absence of any externally defined potential or current, unlike oscillations reported for 180DWs.^{32,33} The resonant frequency was altered by an applied longitudinal field, which changed the equilibrium length of the 360DW. A positive field compressed the 360DW and raised the oscillation frequency.

Figure 4(b) shows how the 360DW oscillation was excited by an ac current over a range of applied fields. An alternating current applied to the 360DW drove an oscillation in the position of the midpoint of the wall at the frequency of the current, as well as an oscillation in the wall length at twice the frequency of the current. When the ac frequency was at or near one-half the resonant frequency of the 360DW, the amplitude of the length oscillation was highest, and when a positive dc magnetic field was simultaneously applied, the resonant frequency increased.

In summary, these simulations predict that the field- and

current-driven behavior of 360DWs differs qualitatively from the behavior of isolated 180DWs. The velocity of a 360DW increased with current density but had no dependence on a field applied parallel to the stripe. 360DWs can therefore move faster or slower than 180DWs at the same current density, depending on the applied field. At sufficient field or current, the 360DW is annihilated, generating spin waves. Furthermore, the 360DW displays an oscillation in its width, which can be excited by an ac current of half the resonant frequency. The resonant frequency can be tuned over a wide range by applying a field along the stripe; for example the 360DW in a $100\text{ nm} \times 5\text{ nm}$ NiFe stripe oscillates at 1.6 GHz at -25 Oe and 3.3 GHz at $+50\text{ Oe}$.

These characteristics are of considerable importance in domain-wall devices, in which interactions between closely spaced 180DWs are likely to create 360DWs, whose subsequent behavior differs dramatically. Additionally, the reso-

nant behavior suggests uses in tunable GHz devices as a possible alternative to spin-torque oscillators. 360DWs could be employed as a vehicle for the delivery of spin-wave energy, e.g., for spin-wave logic devices,^{34,35} by translating the 360DW then annihilating it with a current pulse, delivering a burst of spin waves. The controlled movement then annihilation of 360DWs also suggests their use as programmable pinning sites in multilayer magnetic structures, in which the stray field from a 360DW can “gate” the movement of a 180DW in an adjacent magnetic layer.²⁴ Finally, this work suggests that the behavior of even more complex walls such as 540° or 720° domain walls, in particular, their resonant behavior, may be a fruitful study.

The authors gratefully acknowledge the support of the Nanoelectronics Research Initiative INDEX Center, the National Science Foundation, and the Singapore-MIT Alliance, and G.S. Beach for useful discussions.

*doublemark@mit.edu

†caross@mit.edu

- ¹S. S. P. Parkin, M. Hayashi, and L. Thomas, *Science* **320**, 190 (2008).
- ²P. Xu, K. Xia, C. Gu, L. Tang, H. Yang, and J. Li, *Nat. Nanotechnol.* **3**, 97 (2008).
- ³D. A. Allwood, G. Xiong, C. C. Faulkner, D. Atkinson, D. Petit, and R. P. Cowburn, *Science* **309**, 1688 (2005).
- ⁴A. Yamaguchi, T. Ono, S. Nasu, K. Miyake, K. Mibu, and T. Shinjo, *Phys. Rev. Lett.* **92**, 077205 (2004).
- ⁵M. Eltschka, M. Wötzel, J. Rhensius, S. Krzyk, U. Nowak, M. Kläui, T. Kasama, R. E. Dunin-Borkowski, L. J. Heyderman, H. J. van Driel, and R. A. Duine, *Phys. Rev. Lett.* **105**, 056601 (2010).
- ⁶M. Hayashi, L. Thomas, Y. B. Bazaliy, C. Rettner, R. Moriya, X. Jiang, and S. S. P. Parkin, *Phys. Rev. Lett.* **96**, 197207 (2006).
- ⁷G. S. D. Beach, C. Knutson, C. Nistor, M. Tsoi, and J. L. Erskine, *Phys. Rev. Lett.* **97**, 057203 (2006).
- ⁸F. Junginger, M. Kläui, D. Backes, U. Rüdiger, T. Kasama, R. E. Dunin-Borkowski, L. J. Heyderman, C. A. F. Vaz, and J. A. C. Bland, *Appl. Phys. Lett.* **90**, 132506 (2007).
- ⁹M. Hayashi, L. Thomas, C. Rettner, R. Moriya, X. Jiang, and S. S. P. Parkin, *Phys. Rev. Lett.* **97**, 207205 (2006).
- ¹⁰G. S. D. Beach, C. Nistor, C. Knutson, M. Tsoi, and J. L. Erskine, *Nature Mater.* **4**, 741 (2005).
- ¹¹A. Thiaville, Y. Nakatani, J. Miltat, and Y. Suzuki, *Europhys. Lett.* **69**, 990 (2005).
- ¹²A. Mougin, M. Cormier, J. P. Adam, P. J. Metaxas, and J. Ferré, *EPL* **78**, 57007 (2007).
- ¹³L. Thomas, M. Hayashi, X. Jiang, R. Moriya, C. Rettner, and S. S. P. Parkin, *Nature (London)* **443**, 197 (2006).
- ¹⁴D. G. Porter and M. J. Donahue, *J. Appl. Phys.* **95**, 6729 (2004).
- ¹⁵M. Hayashi, L. Thomas, C. Rettner, R. Moriya, and S. S. P. Parkin, *Nat. Phys.* **3**, 21 (2007).
- ¹⁶M. Kläui, P.-O. Jubert, R. Allenspach, A. Bischof, J. A. C. Bland, G. Faini, U. Rüdiger, C. A. F. Vaz, L. Vila, and C. Vouille, *Phys. Rev. Lett.* **95**, 026601 (2005).
- ¹⁷H. Murakami, K. Takahashi, T. Komine, and R. Sugita, *J. Phys.: Conf. Ser.* **200**, 042018 (2010).
- ¹⁸E. Golovatski and M. Flatté, [arXiv:0909.3831](https://arxiv.org/abs/0909.3831) (unpublished).
- ¹⁹A. Kubetzka, O. Pietzsch, M. Bode, and R. Wiesendanger, *Phys. Rev. B* **67**, 020401(R) (2003).
- ²⁰A. Kunz, *Appl. Phys. Lett.* **94**, 132502 (2009).
- ²¹F. J. Castaño, C. A. Ross, A. Eilez, W. Jung, and C. Frandsen, *Phys. Rev. B* **69**, 144421 (2004).
- ²²G. D. Chaves-O’Flynn, D. Bedau, E. Vanden-Eijnden, A. D. Kent, and D. L. Stein, *IEEE Trans. Magn.* **46**, 2272 (2010).
- ²³X. Portier and A. K. Petford-Long, *Appl. Phys. Lett.* **76**, 754 (2000).
- ²⁴M. D. Mascaro, C. Nam, and C. A. Ross, *Appl. Phys. Lett.* **96**, 162501 (2010).
- ²⁵C. B. Muratov and V. V. Osipov, *J. Appl. Phys.* **104**, 053908 (2008).
- ²⁶F. J. Castaño, C. A. Ross, C. Frandsen, A. Eilez, D. Gil, H. I. Smith, M. Redjda, and F. B. Humphrey, *Phys. Rev. B* **67**, 184425 (2003).
- ²⁷M. Donahue and D. Porter, OOMMF User’s Guide, Version 1.0, National Institute of Standards and Technology, Gaithersburg, MD (September 1999).
- ²⁸S. Zhang and Z. Li, *Phys. Rev. Lett.* **93**, 127204 (2004).
- ²⁹M. T. Bryan, T. Schrefl, D. Atkinson, and D. A. Allwood, *J. Appl. Phys.* **103**, 073906 (2008).
- ³⁰P. E. Roy, T. Trypiniotis, and C. H. W. Barnes, *Phys. Rev. B* **82**, 134411 (2010).
- ³¹M. Shamsutdinov and V. Nazarov, *Phys. Met. Metallogr.* **107**, 569 (2009).
- ³²M. Franchin, T. Fischbacher, G. Bordignon, P. de Groot, and H. Fangohr, *Phys. Rev. B* **78**, 054447 (2008).
- ³³E. Saitoh, H. Miyajima, T. Yamaoka, and G. Tatara, *Nature (London)* **432**, 203 (2004).
- ³⁴A. Khitun and K. L. Wang, *Superlattices Microstruct.* **38**, 184 (2005).
- ³⁵T. Schneider, A. A. Serga, B. Leven, B. Hillebrands, R. L. Stamps, and M. P. Kostylev, *Appl. Phys. Lett.* **92**, 022505 (2008).